

## **Effect of excess Na contents in precursor on the property of Na<sub>2</sub>Zn<sub>2</sub>TeO<sub>6</sub> ceramic solid electrolyte**

Akihiro Itaya, Kazuki Yamamoto, Ryoji Inada\*, Yoji Sakurai

Department of Electrical and Electronic Information Engineering, Toyohashi University of Technology,  
1-1 Hibarigaoka, Tempaku-cho, Toyohashi, Aichi 441-8580, Japan.

\*Corresponding author:

Phone: +81-532-44-6723, Fax: +81-532-44-6757, E-mail address: inada.ryoji.qr@tut.jp

### **Abstract**

We investigated the effect of excess Na contents in precursor on the property of Na<sub>2</sub>Zn<sub>2</sub>TeO<sub>6</sub> (NZTO) solid electrolyte synthesized via a conventional solid state reaction method. In XRD analysis, we confirmed that P2-type layered NZTO phase were mainly formed in all sintered samples, but the samples without excess Na addition in the precursor contained the secondary phases, which could be formed by Na volatilization during high temperature processing. The relative densities of sintered NZTO samples were in the range from 80 to 87% and decreased with increasing the excess Na contents in the precursor. The samples with 0 and 3% excess Na showed the total (grain + grain boundary) conductivity far below 10<sup>-4</sup> S cm<sup>-1</sup> at room temperature, but the conductivity for the samples with 7 and 10% excess Na was well above 10<sup>-4</sup> S cm<sup>-1</sup>. The sample with 7% excess Na in precursor showed the highest conductivity of 3.8 × 10<sup>-4</sup> S cm<sup>-1</sup> at room temperature and low activation energy of 0.25 eV.

**Keywords:** solid electrolyte, layered oxide, sodium-ion conductivity, ceramic

### **1. Introduction**

All-solid-state sodium (Na) ion batteries (SiBs) are promising high-safety and low cost alternatives to current lithium (Li) ion batteries (LiBs), particularly for large-scale energy storage systems [1–4]. Development of inorganic solid Na ion conducting materials for the use as solid electrolyte is most critical issue to realize all-solid-state SiBs. The materials used for solid electrolyte must have not only high Na ion conductivity above 10<sup>-3</sup> S cm<sup>-1</sup> at room temperature but also chemical stabilities against both cathode and anode materials, air and moisture. Although oxide based solid electrolyte materials have rather lower conductivity than sulfide based one, they have other advantages such as their chemical stability and

handling [3, 4].

Na ion conducting oxide  $\text{Na}_2\text{Zn}_2\text{TeO}_6$  (NZTO) have attracted much attention for the application to all-solid-state SiBs, because of the high ionic conductivity above  $10^{-4} \text{ S cm}^{-1}$  at room temperature range and excellent chemical and electrochemical stability [5–9]. In addition, the processing temperature of NZTO is much lower than other Na-ion conducting oxide such as Na- $\beta/\beta'$  alumina [10–12] and NASICON-type  $\text{Na}_3\text{Zr}_2\text{Si}_2\text{PO}_{12}$  [13–15]. NZTO has a honeycomb-structured compound with a space group of  $\text{P6}_3\text{22}$  and in the layers, every  $\text{TeO}_6$  octahedron is surrounded by six  $\text{ZnO}_6$  octahedra via edge-sharing. Na ions are located between the layers at three different sites, all of which are partially occupied and thus Na ions can migrate among them.

In general, Na in the precursor materials is easy to volatilize in high temperature processing. In order to compensate Na loss during high temperature sintering and suppress the secondary phase formation for NZTO, pelletized NZTO samples are covered by the NZTO mother powder, as reported previously [7, 9]. Since this mother powder is difficult to be reused, this process leads to lowering the material yield and increasing the production costs of NZTO. In this paper, we prepared NZTO solid electrolytes with different excess Na contents in the precursor materials by a solid state reaction method. We don't use mother NZTO powder for covering the pellets at sintering process. The effect of excess Na contents in the precursor on the crystal phase, microstructure and ionic conducting property for NZTO were investigated.

## 2. Experimental

NZTO with different excess Na contents of 0 to 10% in the precursor was synthesized via a simple solid state reaction method.  $\text{Na}_2\text{CO}_3$  (Kojundo Chemical Laboratory, 99.5%), ZnO (Kishida Chemical, 99.99%) and  $\text{TeO}_2$  (Kojundo Chemical Laboratory, 99.9%) weighed with the molar ratio of Na : Zn : Te =  $2x : 2 : 1$  ( $x = 1, 1.03, 1.07$  and  $1.10$ ) were mixed and ground with ethanol for 5 hours by planetary ball-milling (Nagao System, Planet M2-3F) with zirconia balls with the diameter of 10 mm, and then calcined at  $850^\circ\text{C}$  for 6 hours in air using a SiC crucible. The calcined powders were reground and pelletized by cold isostatic pressing at 300 MPa and then sintered at  $850^\circ\text{C}$  for 12 hours in air using a SiC crucible.

The density of each sintered NZTO sample was evaluated using the mass and geometrical parameter. The relative density was roughly calculated by dividing the mass density by the theoretical density ( $= 4.88 \text{ g cm}^{-3}$ ) of NZTO [6, 7]. The crystal phase of the composite pellet was evaluated by X-ray diffraction (XRD,

RIGAKU Multiflex) using  $\text{CuK}\alpha$  radiation ( $\lambda = 0.15418$  nm). Fractured surface microstructure of each sintered pellet was observed by a scanning electron microscope (SEM, Keyence VE-8800). The chemical composition of each sintered NZTO were evaluated by inductively coupled plasma optical emission spectroscopy (ICP-OES) analysis. Ionic conductivity was evaluated at a temperature range from 27 to 152°C by an AC impedance measurement with a frequency from 4 Hz to 2 MHz and an applied voltage amplitude of 0.1 V, using an impedance meter (HIOKI IM3536). Before the conductivity measurements, both parallel surfaces of the sintered NZTO pellet were coated with lithium-ion blocking Au electrodes.

### 3. Results and discussion

Fig. 1(a) shows XRD patterns for all sintered NZTO samples with different excess Na contents in the precursor. The patterns for NZTO calculated from the structure data is also plotted as the reference [6]. Although the diffraction peaks of the crystal plane with a  $c$ -axis orientation is slightly emphasized (Fig. 1(a)), the peak position from main phase for all NZTO samples agree well with the peaks of calculated pattern for NZTO. Enlarged diffraction patterns at  $2\theta = 10\text{--}40^\circ$  for all NZTO samples are shown in Fig. 1(b). The sample without excess Na addition in the precursor contains the many small diffraction peaks from secondary phases such as  $\text{Na}_2\text{O}$ ,  $\text{Na}_2\text{O}_2$ ,  $\text{NaOH}$  and  $\text{ZnO}$ . Although the peaks from  $\text{Na}_2\text{O}$  and  $\text{NaOH}$  phases are also detected in samples with excess Na addition, the peak intensity for  $\text{ZnO}$  phase is greatly reduced by excess Na addition in the precursor.

For further examination, we also evaluated the chemical compositions for the samples with 0% and 7% excess Na using ICP-OES analysis and confirmed the molar ratio of  $\text{Na} : \text{Zn} : \text{Te} = 1.91 : 2.00 : 0.95$  for 0% excess Na and  $2.02 : 2.00 : 0.95$  for 7% excess Na, respectively. This indicates that Na is volatilized from NZTO during sintering processing. The Na content in the former is smaller than the stoichiometric one, resulting into the formation of  $\text{ZnO}$  phase in the sample without excess Na addition in the precursor. The volatilization of Na is caused by both the temperature ( $= 850^\circ\text{C}$ ) and duration time ( $= 12$  hours) for sintering used in this work and Na loss during fabrication process is estimated to be approximately 5–6% comparing to the nominal composition in the precursor. Therefore, the proper amount of excess Na addition to compensate the Na loss is necessary for the suppression of the secondary phase formation. If the sintering temperature of NZTO is increased for further densification, it is expected that Na loss becomes more significant and the amount of  $\text{ZnO}$  phase increases.

SEM images of fractured cross sectional surface for sintered NZTO samples with different excess Na contents in the precursor are summarized in Fig. 2. The relative density of each sample was also described in each image. As shown in Fig. 2(a) and (b), the samples with 0% and 3% excess Na in the precursor contain large grains with the size of 10  $\mu\text{m}$ . On the other hand, as shown in Fig. 2(c) and (d), the samples are composed of small grains with size of 2–5  $\mu\text{m}$  and have more porous structure compared to the samples with 0% and 3% excess Na. The relative densities of sintered NZTO tend to decrease as the excess Na contents in the precursor increases. The relation between the grain sizes, pellet densities and the amount of secondary phases in sintered NZTO has not been fully clarified yet, but ZnO phase formed by Na volatilization in the pellet with 0% and 3% excess Na in the precursor may play a role as a sintering aid and increase the pellet densities [16].

Fig. 3 shows the Nyquist plots for electrochemical impedance for all sintered NZTO at 27°C. Here,  $Z'$  in a horizontal axis and  $Z''$  in a vertical axis are the real and imaginary parts of impedance and the units for both components are  $\Omega\text{ cm}$ , for direct comparison among the samples with different geometrical parameters. As shown in Fig. 3(a), the plots for the samples with 0% and 3% excess Na in the precursor are composed of the part of a semicircle at frequency above 0.5 MHz, a distorted semicircle at frequency range between several 100 Hz to 0.5 MHz and a linear tail at low frequency range below several 100 Hz. These data belong to the ionic conduction in NZTO grains, the ionic conduction at NZTO grain boundaries and the response by ionic blocking electrodes, respectively. The intercept point of an extrapolation line of the linear tail in low frequency range and horizontal  $Z'$  axis corresponds to the total (grain + grain boundary) resistance  $R_{\text{total}}$  of the sample. For these two samples, it is confirmed that grain boundary resistance (corresponding to the diameter of a semicircle observed at several 100 Hz to 0.5 MHz) is dominant component in  $R_{\text{total}}$ . We believe that the secondary phases contained in NZTO with 0% and 3% excess Na in the precursor severely interfere with Na ion conduction at grain boundaries. Similar results have been observed in our previous work for perovskite-type Li ion conducting oxide  $\text{Li}_{3/8}\text{Sr}_{7/16}\text{Ta}_{3/4}\text{Zr}_{1/4}\text{O}_3$  (LSTZO) without excess Li addition in the precursor, which contains small amount of both  $\text{SrTa}_2\text{O}_6$  and  $\text{Sr}_2\text{Ta}_2\text{O}_7$  phases formed by the volatilization of Li in sintering process [17, 18]. These secondary phases are mainly formed on the surface of LSTZO grains and increase the grain-boundary resistance significantly. On the other hand, although the relative densities for the samples with 7 and 10% excess Na contents in the precursor are smaller than those for the samples with 0 and 3% excess Na, the  $R_{\text{total}}$  for the former is approximately one order smaller than for the

latter (Fig. 3(b)), which is mainly attributed to the improvement in ionic conduction property due to the reduction of secondary phases.

Total (grain + grain boundary) ionic conductivity  $\sigma_{\text{total}}$  of each NZTO sample is calculated by the  $R_{\text{total}}$  value estimated in Fig. 3. Fig. 4(a) shows variation of the product of  $\sigma_{\text{total}}$  and measurement temperature  $T$  for all sintered NZTO as a function of inverse of temperature  $1000/T$ . The magnitude relationship of  $\sigma_{\text{total}}$  among the samples does not change within the measurement temperature range. In addition, the temperature dependence of  $\sigma_{\text{total}}$  is well expressed by the Arrhenius equation  $\sigma_{\text{total}}T = \sigma_0 \exp(-E_a / k_B T)$ . Here,  $\sigma_0$  is constant,  $E_a$  is activation energy of conductivity and  $k_B$  is Boltzmann constant ( $= 1.381 \times 10^{-23} \text{ J K}^{-1}$ ), respectively.  $E_a$  of each sample can be estimated from the slope of  $\sigma_{\text{total}}T$  plotted in Fig. 4(a).  $\sigma_{\text{total}}$  at 27°C and  $E_a$  for sintered NZTO are also shown in Fig. 4(b), as a function of the excess Na contents in the precursor. The samples with excess Na contents of 0 and 3% in the precursor showed  $\sigma_{\text{total}}$  far below  $10^{-4} \text{ S/cm}$  at room temperature, and the sample without excess Na addition in the precursor has the lowest  $\sigma_{\text{total}} = 0.22 \times 10^{-4} \text{ S cm}^{-1}$  and the highest  $E_a = 0.31 \text{ eV}$ . This is mainly due to the presence of secondary phases in the sample. On the other hand, the conductivity for the samples with 7 and 10% excess Na was well above  $10^{-4} \text{ S/cm}$ , which is mainly attributed to the suppression of secondary phase formation by the Na volatilization in sintering process. In our experiments, the sample with 7% excess Na in precursor showed the highest  $\sigma_{\text{total}} = 3.8 \times 10^{-4} \text{ S cm}^{-1}$  at room temperature and low  $E_a = 0.25 \text{ eV}$ . This value is comparable to the value for NZTO sintered with mother powder [7, 9]. The sample with excess Na content of 10% has slightly lower  $\sigma_{\text{total}} = 2.6 \times 10^{-4} \text{ S cm}^{-1}$  than the sample with excess Na content of 7%, which may be attributed to the lowest relative density (= 79%).

#### 4. Conclusion

We investigated the effect of excess Na contents in precursor on the property of NZTO solid electrolyte prepared by a solid state reaction method. XRD data showed that P2-type layered NZTO phase was mainly formed in all sintered samples. However, the samples with 0% and 3% excess Na in precursor contained small amount of secondary phases, which could be formed by the volatilization Na during high temperature processing. In our experiments, the total conductivity sintered NZTO samples with 7 and 10% excess Na in precursor was well above  $10^{-4} \text{ S/cm}$  at room temperature and the sample with 7% excess Na showed the

highest room temperature conductivity of  $3.8 \times 10^{-4}$  S/cm at and low activation energy of 0.25 eV. Proper choice of excess Na contents in the precursor is crucial to achieve high ionic conductivity in sintered NZTO.

### Acknowledgements

This work was partly supported by Iketani Science and Technology Foundation, Japan and Foundation of Public Interest of Tatematsu, Japan. ICP-OES analysis for all sintered NZTO samples was carried out at Izumitec Co., Ltd, Toyohashi, Aichi, Japan. We acknowledged the support of the Cooperative Research Facility Center at Toyohashi University of Technology.

### References

- [1] W. Zhou, Y. Li, S. Xin, J.B. Goodenough, *ACS Cent. Sci.* 3 (2017) 52–57.
- [2] W. Hou, X. Guo, X. Shen, K. Amine, H. Yu, J. Lu, *Nano Energy* 52 (2018) 279–291.
- [3] C. Zhou, S. Bag, V. Thangadurai, *ACS Energy Lett.* 3 (2018) 2181–2198.
- [4] Q. Ma, F. Tietz, *ChemElectroChem* 7 (2020) 2693–2713.
- [5] M.A. Evstigneeva, V.B. Nalbandyan, A.A. Petrenko, B.S. Medvedev, A.A. Kataev, *Chem. Mater.* 23 (2011) 1174–1181.
- [6] Y. Li, Z. Deng, J. Peng, E. Chen, Y. Yu, X. Li, J. Luo, Y-Y. Huang, J. Zhu, C. Fang, Q. Li, J. Han, *Chem. Eur. J.* 24 (2018) 1057–1061.
- [7] J-F. Wu, Q. Wang, X. Guo, *J. Power Sources* 402 (2018) 513–518.
- [8] Z. Deng, J. Gu, Y. Li, S. Li, J. Peng, X. Li, J. Luo, Y-Y. Huang, C. Fang, Q. Li, J. Han, Y. Huang, Y. Zhao, *Electrochimica Acta* 298 (2019) 121–126.
- [9] X. Li, F. Bianchini, J. Wind, C. Pettersen, D.S. Wragg, P. Vajeeston, H. Fjellvåg, *ACS Appl. Mater. Interfaces* 12 (2020) 28188–28198.
- [10] G.E. Youngblood, G.R. Miller, R.S. Gordon, *J. Am. Ceram. Soc.* 61 (1978) 86–87.
- [11] X. Lu, G. Xia, J.P. Lemmon, Z. Yang, *J. Power Sources* 195 (2010) 2431–2442.
- [12] M-C. Bay, M. Wang, R. Glissa, M.V.F. Heinz, J. Sakamoto, C. Battaglia, *Adv. Energ. Mater.* 10 (2020) 1902899.
- [13] J.B. Goodenough, H.Y-P. Hong, J.A. Kafalas, *Mater. Res. Bull.* 11 (1976) 203–220.
- [14] S. Narayanan, S. Reid, S. Butler, V. Thangadurai, *Solid State Ionics* 331 (2019) 22–29.

- [15] Q. Ma, C-L. Tsai, X-K. Wei, M. Heggen, F. Tietz, J.T.S. Irvine, *J. Mater. Chem. A* 7 (2019) 7766–7776.
- [16] A. Sedky, T.A.El-Brolossy, S.B.Mohamed, *J. Phys. Chem. Solids* 73 (2012) 505–510.
- [17] R. Inada, K. Kimura, K. Kusakabe, T. Tojo, Y. Sakurai, *Solid State Ionics* 261 (2014) 95–99.
- [18] K. Kimura, K. Wagatsuma, T. Tojo, R. Inada, Y. Sakurai, *Ceramic International* 42 (2016) 5546–5552.

Figures with captions

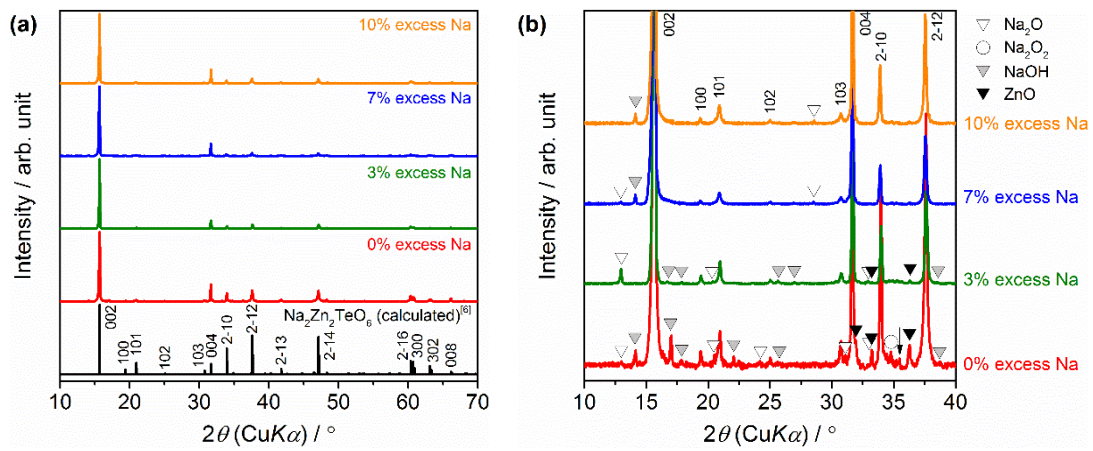


**Fig. 1.** (a) XRD patterns of sintered NZTO with different Na contents in the precursor. Enlarged diffraction patterns at  $2\theta = 10\text{--}40^\circ$  are also shown in (b).  $\text{Na}_2\text{O}$ ,  $\text{Na}_2\text{O}_2$ ,  $\text{NaOH}$  and  $\text{ZnO}$  are detected as secondary phases. The peak from unidentified phase is marked with an arrow.

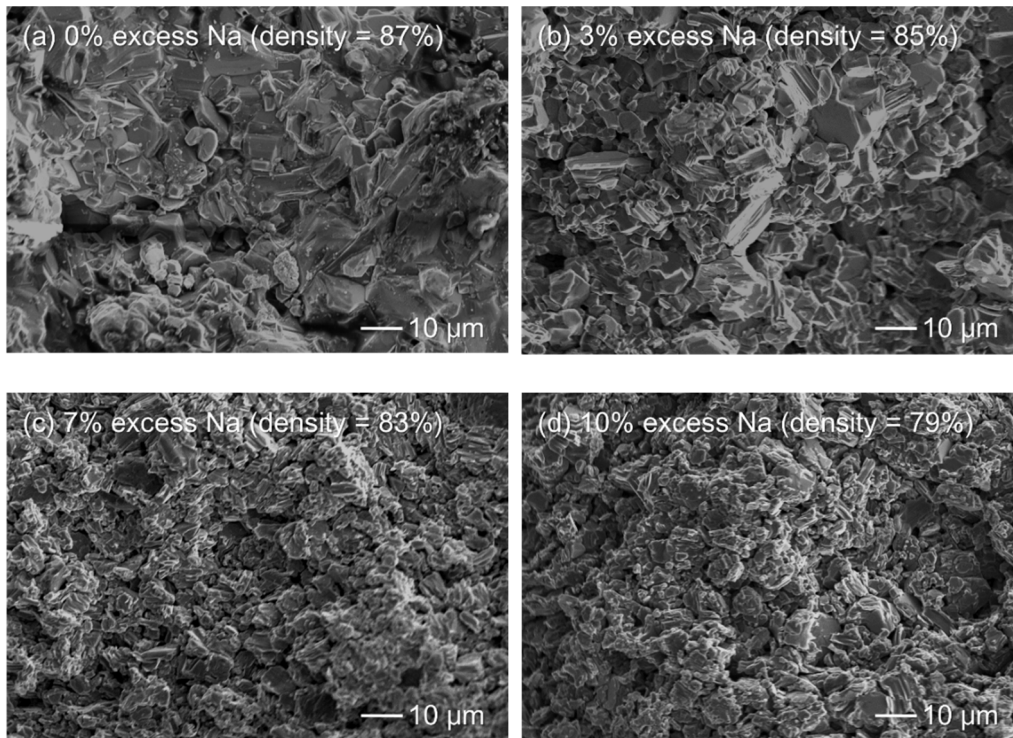


**Fig. 2.** SEM images for fractured surface microstructures of sintered NZTO with different excess Na contents in the precursor. The relative density of each sample is also shown in the image.

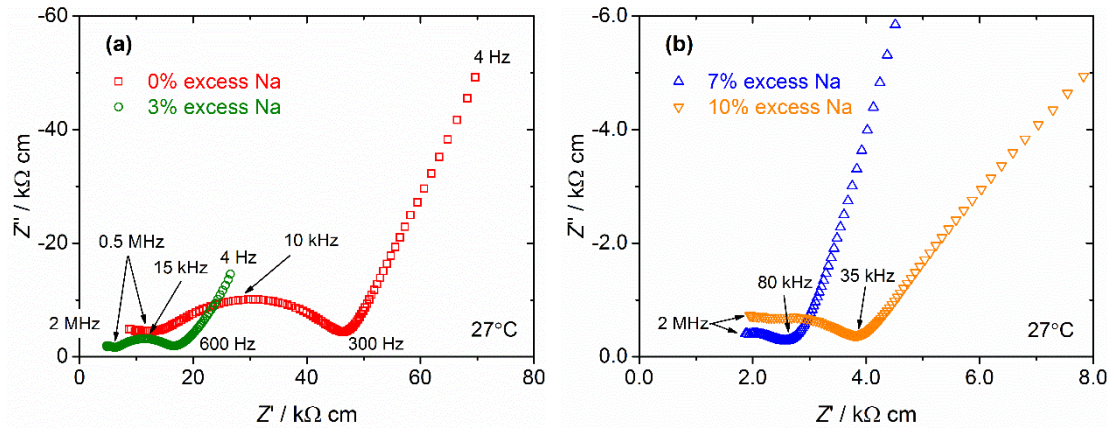


**Fig. 3.** Nyquist plots of AC impedance at 27°C for sintered NZTO with different excess Na contents in the precursor: (a) 0% and 3% and (b) 7% and 10%.

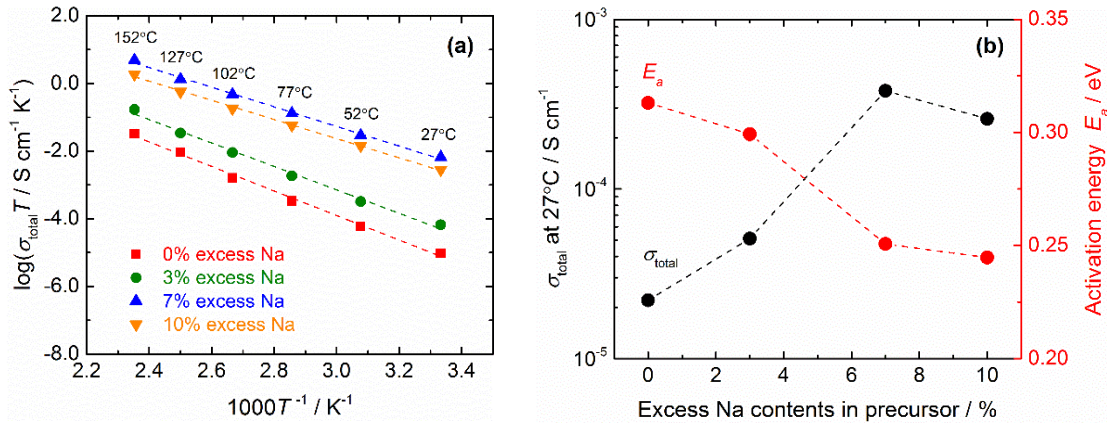


**Fig. 4.** (a) Arrhenius plots for all sintered NZTO with different excess Na contents in the precursor. The conductivity at 27°C and activation energy for NZTO are also shown in (b), plotted against the excess Na contents in the precursor.